

## Conformational Behavior of Norephedrine, Ephedrine, and Pseudoephedrine

José L. Alonso,\* M. Eugenia Sanz, Juan C. López, and Vanessa Cortijo

*Grupo de Espectroscopia Molecular (GEM), Departamento de Química Física y Química Inorgánica, Facultad de Ciencias, Universidad de Valladolid, 47005 Valladolid, Spain*

Received October 3, 2008; E-mail: jlalonso@qf.uva.es

**Abstract:** A conclusive identification of the different conformers of the neurotransmitters ephedrine, norephedrine, and pseudoephedrine has been carried out in the gas-phase by molecular beam Fourier transform microwave (MB-FTMW) spectroscopy. Three conformers of norephedrine, three conformers of ephedrine, and four conformers of pseudoephedrine have been unequivocally assigned through the analysis of their rotational spectra and the comparison of the experimental rotational and  $^{14}\text{N}$  quadrupole coupling constants with those calculated ab initio. The conformational preferences have been rationalized in terms of the various intramolecular forces at play. The main stabilizing interaction is an  $\text{O}\cdots\text{N}$  hydrogen bond established in the side chain of the neurotransmitters which adopt an extended disposition in their most stable form.

### I. Introduction

Molecular shape has a matchless influence in acceptor–receptor interactions in biological processes. Active sites in receptors and enzymes are chiral and interact only with molecules of the correct conformation. The several enantiomers or stereoisomers of a chiral molecule have the same empirical formula but behave differently and can produce distinct physiological effects. Furthermore, each enantiomer or stereoisomer can adopt different conformations depending on its flexibility. In this case, knowledge of the various conformers is relevant to understand the selectivity of the biological processes in which the chiral molecule participates as one of its conformers may interact preferentially with the receptor. In the physiological medium the inherent conformational preferences of the isolated molecule can be altered by interactions with water molecules and by the pH of the medium, which may induce protonation in the molecule of interest or in adjacent sites.<sup>1,2</sup> A thorough understanding of the forces affecting conformational preferences should be built up from the study of the isolated molecule to increasing levels of complexity.

An example of flexible chiral molecules with distinctive physiological effects is illustrated by the phenylpropanolamines norephedrine ( $\text{C}_6\text{H}_5\text{—CHOH—CHNH}_2\text{—CH}_3$ ), ephedrine and pseudoephedrine ( $\text{C}_6\text{H}_5\text{—CHOH—CHNH(CH}_3\text{)—CH}_3$ ). They all possess two chiral carbons which differ in the stereochemistry around them. Ephedrine and pseudoephedrine are stereoisomers which derive from substitution of a hydrogen atom by a methyl group in norephedrine, and they differ in the stereochemistry of one chiral center. Thus, six stereoisomers arise, two for each molecule, of which only (1*R*,2*S*)-norephedrine (NEP), (1*R*,2*S*)-ephedrine (EP), and (1*S*,2*S*)-pseudoephedrine (PEP, see chart

1) are found in nature,<sup>3</sup> more specifically in the Ephedra species of plants. When introduced in humans, these biologically active molecules act directly on the sympathetic nervous system by altering the natural neurotransmission process. Their mechanism of action is similar, but their pharmacological behavior differs. EP is the most potent stimulant,<sup>3,4</sup> and it is used as a bronchodilator, vasoconstrictor, and cardiac stimulator. PEP is mainly employed in flu treatment as a descongostant, and NEP is used as an appetite suppressor and in cold and cough medications. The distinct physiological effects produced by these phenylpropanolamines are directly related to their structure. Hence, the investigation of the preferred conformations of these neurotransmitters and the intramolecular interactions responsible for their stabilization becomes relevant. The experimental studies should be conducted under isolation conditions in the gas phase where no intermolecular interactions can alter the natural conformational preferences.

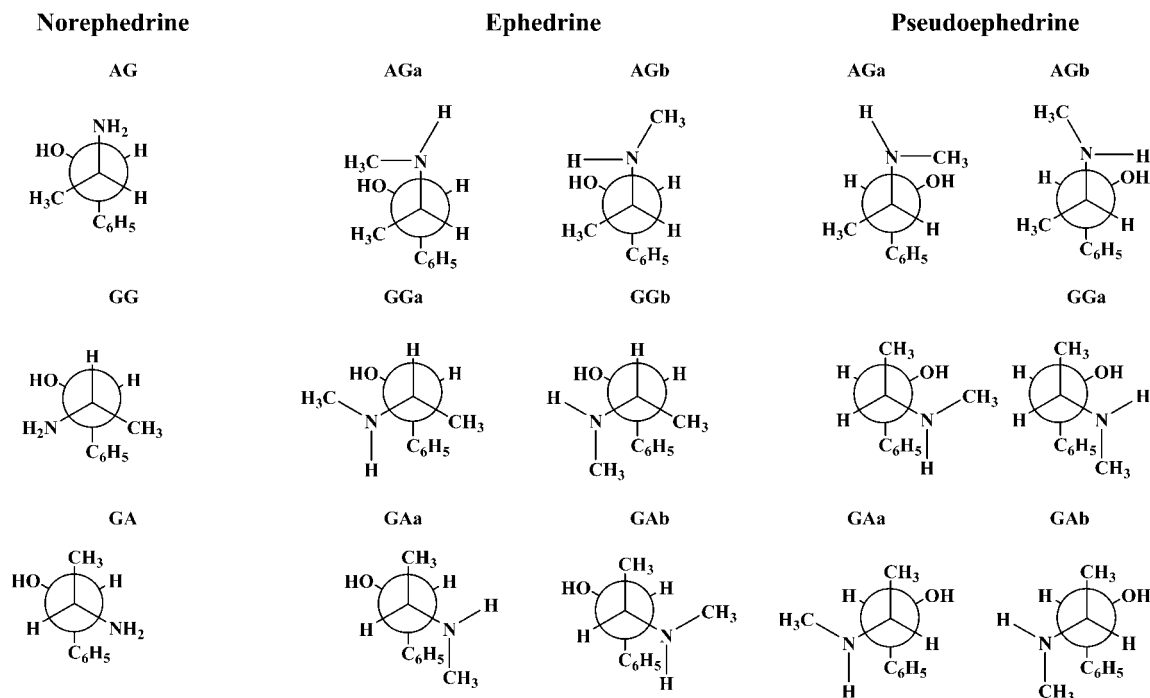
NEP, EP, and PEP of chart 1 are expected to present different conformations due to the flexibility of its ethanolamine side chain. The plausible configurations are labeled with two indexes, A or G, that indicate anti or gauche arrangement of the CCCN chain (first index) and the OCCN chain (second index). Thus, three possible conformations arise in NEP: AG, GG, and GA forms. In PE and PEP, where one of the H atoms of the amino group is replaced by a  $\text{—CH}_3$ , the number of conformations increases since two nonequivalent positions for the methyl group (labeled a and b) are possible. Previous spectroscopic studies of these three neurotransmitters in the gas phase have taken advantage of the phenyl ultraviolet chromophore. Butz et al.<sup>5,6</sup> obtained their electronic and IR spectra using resonant two-photon ionization (R2PI), laser induced fluorescence (LIF), and

(1) Blom, M. N.; Compagnon, I.; Polfer, N. C.; von Helden, G.; Meijer, G.; Suhai, S.; Paizs, B.; Oomens, J. *J. Phys. Chem. A* **2007**, *111*, 7309.  
 (2) Simons, J. P. C. R. *Chim.* **2003**, *6*, 17.

(3) Abourashed, E. A.; El-Alfy, A. T.; Khan, I. A.; Walker, L. *Phytother. Res.* **2003**, *17*, 703.

(4) Vansal, S. S.; Feller, D. R. *Biochem. Pharmacol.* **1999**, *58*, 807.

(5) Butz, P.; Kroemer, R. T.; Macleod, N. A.; Robertson, E. G.; Simons, J. P. *J. Phys. Chem. A* **2001**, *105*, 1050.

Chart 1. Newman Projections of (1*R*,2*S*)-Norephedrine, (1*R*,2*S*)-Ephedrine, and (1*S*,2*S*)-Pseudoephedrine<sup>a</sup>

<sup>a</sup> The A/G notation refers to the anti or gauche arrangement of the C<sub>arom</sub>CCN and OCCN chains, respectively. The three different substituent groups on the N atom result in a further distinction (a or b) between the (nonequivalent) structures generated by the rotation of the methylamino group.

resonant ion-dip infrared spectroscopy (RIDIRS). In combination with high-level quantum chemical calculations, the authors used such techniques to probe the conformational landscape of the neurotransmitters. They explored the hydrogen-bonding nature of the -OH and -NH groups and discussed in detail the intramolecular interactions identified through vibrational data in the isolated ephedras. Two origin bands in the spectrum of NEP were interpreted in terms of the presence of two conformers (AG and GG) of the three low-lying conformers predicted (see Chart 1).<sup>5</sup> Four conformers of PEP were found to be present. For EP<sup>6</sup> two of its low-lying conformers were detected (AGa and AGb), but surprisingly the conformer GGa, lying at an intermediate energy, was not. A weak transition moment or/and the lack of facile relaxation pathways from higher conformers to GGa were proposed to explain this "missing" conformer in the supersonic expansion. From the data obtained the authors concluded that the main stabilizing force for all conformers of NEP, EP, and PEP is a hydrogen bond between the hydroxyl and the amide group in the side chain. More recently Chervenkov et al.<sup>7</sup> carried out low- and high-resolution resonantly enhanced two-photon ionization spectroscopic studies with mass selection on a mixture of EP and water, which led to the conclusion that there exist three different species in the molecular beam: one form of ephedrine-water and two distinct conformers of ephedrine. The high-resolution spectrum of the strongest vibronic peak yielded the values of the rotational constants for the ground and excited states of the AGa conformer. The authors conclude that high-resolution spectroscopy

copy data are needed to obtain undeniable data on the conformational preferences of ephedrine and other neurotransmitters.

Unlike the techniques mentioned above, microwave spectroscopy can distinguish unambiguously between different conformational structures and provide accurate structural information directly comparable to the in vacuo theoretical predictions. The various populated conformers possess distinct rotational spectra and can thus be unequivocally identified. The combination of microwave spectroscopy with supersonic jets<sup>8</sup> has proved to be a powerful tool in the investigation of the conformational behavior of biomolecular systems in the gas phase.<sup>9–12</sup> Moreover, small hyperfine structure arising from <sup>14</sup>N nuclear quadrupole effects can be fully resolved. For conformers showing only slight geometry changes, conclusive evidence for their identification comes from the values of <sup>14</sup>N quadrupole coupling constants, which are very sensitive to the orientation of the amino group with respect to the principal axis system.<sup>12–14</sup> Because the amino group is expected to be involved in the intramolecular interactions (hydrogen bonds) that drive conformational preferences, knowing its disposition relative to the rest of the molecule allows the nature of those interactions to be derived.

- (6) (a) Butz, P.; Kroemer, R. T.; Macleod, N. A.; Robertson, E. G.; Simons, J. P. *J. Phys. Chem. A* **2001**, *105*, 544. (b) Butz, P.; Macleod, N. A.; Talbot, L. C.; Snoeck, F. O.; Simons, J. P. *Central Laser Facility Report* **2000/2001**, 97.  
 (7) Chervenkov, S.; Wang, P. Q.; Braun, J. E.; Neuser, H. J. *J. Chem. Phys.* **2004**, *121*, 7169.

- (8) Balle, T. J.; Flygare, W. H. *Rev. Sci. Instrum.* **1981**, *52*, 33.  
 (9) Blanco, S.; Sanz, M. E.; López, J. C.; Alonso, J. L. *Proc. Natl. Acad. Sci. U.S.A.* **2007**, *104*, 20183, and references therein.  
 (10) Sanz, M. E.; Blanco, S.; López, J. C.; Alonso, J. L. *Angew. Chem., Int. Ed.* **2008**, *47*, 6216.  
 (11) Blanco, S.; López, J. C.; Alonso, J. L.; Ottaviani, P.; Caminati, W. *J. Chem. Phys.* **2003**, *119*, 880.  
 (12) Alonso, J. L.; Pérez, C.; Sanz, M. E.; López, J. C.; Blanco, S. *Phys. Chem. Chem. Phys.* **2009**, *11*, 617.  
 (13) Sanz, M. E.; Lesarri, A.; Peña, M. I.; Vaquero, V.; Cortijo, V.; López, J. C.; Alonso, J. L. *J. Am. Chem. Soc.* **2006**, *128*, 3812.  
 (14) López, J. C.; Cortijo, V.; Blanco, S.; Alonso, J. L. *Phys. Chem. Chem. Phys.* **2007**, *9*, 4521.

On this basis, we have tackled the problem of determining the conformations of NEP, EP, and PEP and the nature of their intramolecular interactions. Analysis of our MB-FTMW spectroscopy data and the comparison of the experimental parameters with those predicted ab initio led to the conclusive identification of three conformers of NEP and EP and four conformers of PEP. The role of the intramolecular interactions between the  $-NH_2$  (or  $-NHCH_3$ ) and  $-OH$  in the side chain and the aromatic  $\pi$  system has been discussed on the basis of the relative abundances of the conformers, derived from relative intensity measurements. The newly detected conformer of NEP is stabilized by a  $N-H\cdots\pi$  hydrogen bond. The detection of the GGa conformer of EP changes the conformational landscape of this neurotransmitter and allows the rationalization of the results obtained for all three neurotransmitters. Details are described in the following sections.

## II. Methods

The rotational spectra of the three neurotransmitters have been investigated using our MB-FTMW spectrometer, described in detail elsewhere.<sup>15</sup> Solid samples of NEP, EP, and PEP were obtained commercially (Sigma-Aldrich, 99%, mp = 52, 36, and 120 °C, respectively) and used without further purification. The three samples were vaporized in our heated nozzle, which has been modified from its previous design<sup>11</sup> to optimize its performance. The heated nozzle now consists of a stainless steel receptacle for the sample attached to the solenoid valve with a special housing for the poppet to improve the supersonic expansion flow. This part screws into a macor insulator element that has been machined to hold the electric resistance and connections for heating. The whole piece is attached in the center of the rear side of one of the Fabry–Pérot mirrors. The optimal temperature for vaporization was found by repeatedly scanning at temperatures between 40 and 130 °C the spectral region around the predicted frequencies. In all cases a good signal-to-noise ratio was achieved with a temperature of about 120 °C.

The vaporized molecules are entrained in several atmospheres of Ne (ca. 7 bar) and pulsed through a 1.0 mm nozzle into a vacuum chamber (where a Fabry–Pérot resonator is placed) to create a supersonic expansion. Here a short microwave pulse polarizes the species in the jet. When the excitation microwave pulse finishes the molecular emission signal containing the rotational transitions is captured in the time domain, and then Fourier-transformed to obtain the frequency domain spectrum. Due to the collinearity between the supersonic jet and the microwave resonator axis, all transitions appear split by the Doppler effect. The resonance frequency is the arithmetic mean of the two Doppler components.

Previous ab initio calculations reported in the literature<sup>5,6</sup> have been extended in order to predict rotational constants, quadrupole coupling constants, and electric dipole moment components relevant for the interpretation of rotational spectra. Geometry optimizations of the lower-energy conformers were carried out at the MP2/6-311++G(d,p) level of theory using the Gaussian03<sup>16</sup> software package. Harmonic frequency calculations were performed to obtain the zero point energies (ZPEs) and to confirm that all predicted conformers are local minima in the potential energy surface. Tables 1, 2, and 3 summarize the calculated parameters for NEP, EP, and PEP, respectively.

**Table 1.** Ab Initio Spectroscopic Constants for the Conformers of Norephedrine Calculated at the MP2/6-311++G(d,p) Level of Theory

	AG	GG	GA
$A^a$ /MHz	2323	1851	2199
$B$ /MHz	683	796	700
$C$ /MHz	644	718	634
$\chi_{aa}$ /MHz	2.52	1.89	1.90
$\chi_{bb}$ /MHz	-4.20	-3.75	1.74
$\chi_{cc}$ /MHz	1.68	1.85	-3.64
$\mu_a$ /D	-1.2	0.3	-1.3
$\mu_b$ /D	2.6	-2.2	0.2
$\mu_c$ /D	-0.8	-2.3	0.5
$E_{MP2}/E_h$	-479.4898594	-479.4892613	-479.4875159
$\Delta E_{MP2}/cm^{-1}$	0	131	514
$\Delta E_{MP2+ZPE}/cm^{-1b}$	0	164	390

<sup>a</sup>  $A$ ,  $B$ , and  $C$  represent the rotational constants;  $\chi_{aa}$ ,  $\chi_{bb}$ , and  $\chi_{cc}$  are elements of the  $^{14}N$  nuclear quadrupole coupling tensor;  $\mu_a$ ,  $\mu_b$ , and  $\mu_c$  are the electric dipole moment components. <sup>b</sup> MP2/6-311++G(d,p) electronic energies corrected with zero-point vibrational energies (ZPE) calculated at the B3LYP/6-311++G(d,p) level.

## III. Rotational Spectra and Assignments

**a. Norephedrine.** Since highly excited rotational states are depopulated at the low rotational temperature achieved in the supersonic expansion, initial scans were directed to search for the most intense transitions with low angular momentum quantum numbers predicted from the values of the rotational constants of Table 1. It was relatively straightforward to identify a set of  $\mu_a$ -type R-branch transitions as belonging to a rotamer close to the prolate symmetric top limit. All transitions appeared split into several hyperfine components, which showed the typical pattern arising from the presence of a species with a single  $^{14}N$  quadrupolar nucleus ( $I = 1$ ). A total of 97 hyperfine components belonging to  $\mu_a$ ,  $\mu_b$ , and  $\mu_c$  R-branch transitions were collected. Analysis of the line frequencies was performed using Watson's semirigid rotor Hamiltonian<sup>17</sup> in the  $I'$  representation,  $H_R$ , supplemented with an additional term,  $H_Q$ , to account for the nuclear quadrupole coupling,<sup>18</sup> that was set up in the coupled basis set ( $IJF$ ),  $I + J = F$ . The tensor describing the quadrupole coupling,  $\chi$ , is related to the molecular electrical field gradient tensor (at the  $^{14}N$  nucleus)  $q$  by  $\chi = eQq$  where  $Q$  represents the  $^{14}N$  nuclear electric quadrupole moment. Only the diagonal elements of the nuclear quadrupole coupling tensor ( $\chi_{aa}$ ,  $\chi_{bb}$ ,  $\chi_{cc}$ ) were necessary to fit<sup>19</sup> the experimental frequencies within the estimated accuracy of the frequency measurements. The resulting spectroscopic constants are shown in column 1 of Table 4. A comparison between the predicted rotational constants of Table 1 for the three conformers of NEP with those of column 1 in Table 4 does not allow an identification of the observed species. The values of  $A$ ,  $B$ , and  $C$  are very similar to those of the AG and GA species but they do not allow a conclusive discrimination. Definitive evidence comes from the values of the  $^{14}N$  quadrupole coupling constants, which markedly change in passing from AG to GA (see Table 1) due to the different orientation of the  $-NH_2$  group in each conformer. The fitted values of the diagonal elements of the  $^{14}N$  quadrupole coupling tensor,  $\chi_{aa}$ ,  $\chi_{bb}$ , and  $\chi_{cc}$ , in Table 2 match nicely those predicted for the AG conformer evidencing the existence of this conformer in the supersonic jet.

(15) Alonso, J. L.; Lorenzo, F. J.; López, J. C.; Lesarri, A.; Mata, S.; Dreizler, H. *Chem. Phys.* **1997**, *218*, 267.

(16) Frisch, M. J.; et al. *Gaussian 03, Revision B.04*, Gaussian, Inc., Pittsburgh PA, 2003.

(17) Watson J. K. G. In *Vibrational Spectra and Structure*; Durig, J. R., Ed.; Elsevier: New York/Amsterdam, 1977; Vol. 6, pp 1–78.

(18) Gordy W.; Cook, R. L. *Microwave Molecular Spectra*, 3rd ed.; John Wiley and Sons: New York, 1984.

(19) Pickett, H. M. *J. Mol. Spectrosc.* **1991**, *148*, 371.

**Table 2.** Ab Initio Spectroscopic Constants for the Conformers of Ephedrine Calculated at the MP2/6-311++G(d,p) Level of Theory

	AGa	GGa	AGb	GAa	GAb	GGb
$A^a$ /MHz	2014	1566	2112	1536	1506	1418
$B$ /MHz	533	597	507	676	615	682
$C$ /MHz	505	579	480	570	524	664
$\chi_{aa}$ /MHz	2.63	2.51	2.70	0.57	1.86	1.30
$\chi_{bb}$ /MHz	-3.26	-2.90	-4.83	2.88	2.88	-4.23
$\chi_{cc}$ /MHz	0.63	0.39	2.14	-3.45	-4.74	2.93
$\mu_a$ /D	1.6	-0.6	-1.5	0.5	-0.6	0.9
$\mu_b$ /D	-2.0	-1.6	2.3	-0.7	-0.1	-2.5
$\mu_c$ /D	-1.6	2.6	-0.2	0.0	-1.6	-1.6
$E_{MP2}/E_h$	-518.6748258	-518.6737476	-518.6727881	-518.6712449	-518.6712129	-518.6702625
$\Delta E_{MP2}/cm^{-1}$	0	236	447	786	793	1002
$\Delta E_{MP2+ZPE}/cm^{-1}{}^b$	0	256	473	644	673	1108

<sup>a</sup>  $A$ ,  $B$ , and  $C$  represent the rotational constants;  $\chi_{aa}$ ,  $\chi_{bb}$ , and  $\chi_{cc}$  are elements of the  $^{14}\text{N}$  nuclear quadrupole coupling tensor;  $\mu_a$ ,  $\mu_b$ , and  $\mu_c$  are the electric dipole moment components. <sup>b</sup> MP2/6-311++G(d,p) electronic energies corrected with zero-point vibrational energies (ZPE) calculated at the B3LYP/6-311++G(d,p) level.

**Table 3.** Ab Initio Spectroscopic Constants for the Conformers of Pseudoephedrine Calculated at the MP2/6-311++G(d,p) Level of Theory

	AGa	GGb	GGa	AGb	GAb	GAa
$A^a$ /MHz	1997	1638	1641	2047	1536	1506
$B$ /MHz	513	616	570	533	676	615
$C$ /MHz	482	595	548	490	570	524
$\chi_{aa}$ /MHz	2.79	1.86	1.60	2.75	0.57	1.86
$\chi_{bb}$ /MHz	-4.44	-0.59	-0.12	-3.98	2.88	2.88
$\chi_{cc}$ /MHz	1.65	-1.26	-1.49	1.23	-3.45	-4.76
$\mu_a$ /D	1.6	0.6	0.1	1.7	-0.5	1.5
$\mu_b$ /D	-2.5	-2.7	-2.6	2.3	-0.7	-0.6
$\mu_c$ /D	0.9	-0.8	-0.9	1.4	0.0	-0.2
$E_{MP2}/E_h$	-518.6742806	-518.673425	-518.6731355	-518.6728403	-518.6712451	-518.6712131
$\Delta E_{MP2}/cm^{-1}$	0	188	251	316	666	673
$\Delta E_{MP2+ZPE}/cm^{-1}{}^b$	0	251	337	367	554	583

<sup>a</sup>  $A$ ,  $B$ , and  $C$  represent the rotational constants;  $\chi_{aa}$ ,  $\chi_{bb}$ , and  $\chi_{cc}$  are elements of the  $^{14}\text{N}$  nuclear quadrupole coupling tensor;  $\mu_a$ ,  $\mu_b$ , and  $\mu_c$  are the electric dipole moment components. <sup>b</sup> MP2/6-311++G(d,p) electronic energies corrected with zero-point vibrational energies (ZPE) calculated at the B3LYP/6-311++G(d,p) level.

**Table 4.** Experimental Rotational and Quadrupole Coupling Constants for the Observed Conformers of Norephedrine (See Table S1 of the Supporting Information for a Complete Set of Parameters)

	AG	GG	GA
$A^a$ /MHz	2330.15332(22) <sup>d</sup>	1856.19039(80)	2210.38150(76)
$B$ /MHz	676.963452(41)	791.01512(14)	696.642553(62)
$C$ /MHz	637.669563(43)	709.15405(14)	627.302876(54)
$\chi_{aa}$ /MHz	2.3837(28)	1.681(19)	1.659(15)
$\chi_{bb}$ /MHz	-3.8821(25)	-3.627(12)	1.7497(99)
$\chi_{cc}$ /MHz	1.4984(25)	1.946(12)	-3.4087(99)
$N^b$	88	33	41
$\sigma^c$ /kHz	1.1	2.1	1.1

<sup>a</sup>  $A$ ,  $B$ , and  $C$  are the rotational constants and  $\chi_{aa}$ ,  $\chi_{bb}$ , and  $\chi_{cc}$  are elements of the  $^{14}\text{N}$  nuclear quadrupole coupling tensor. <sup>b</sup> Number of fitted hyperfine components. <sup>c</sup> rms deviation of the fit. <sup>d</sup> Standard error in parentheses in units of the last digit.

During the analysis of the rotational spectrum of conformer AG a set of weaker  $\mu_a$ -type transitions was observed very close in frequency to those of conformer AG, exhibiting  $^{14}\text{N}$  hyperfine structure. These transitions were assigned to the spectrum of another rotamer. The assignment was completed with measurements of  $\mu_c$ -type R-branch transitions. A total of 54 components were fitted using the same Hamiltonian described above to give the rotational constants of column 2 of Table 4. The excellent

match between experimental and predicted (Table 1) values of rotational and quadrupole coupling constants allows the identification of the observed spectrum as belonging to conformer GA. Additional frequency scans were then performed trying to detect the GG form in the supersonic expansion. After discarding all the signals arising from transitions of conformers AG and GA,  $a$ -,  $b$ -, and  $c$ -type R-branch transitions from a new rotamer were identified, whose analysis yielded the spectroscopic constants in column 3 of Table 4. Their comparison with those predicted theoretically (Table 1) allows us to assign the observed species to the GG conformer.

For the three conformers of NEP, the ab initio rotational constants of Table 1 are in very good agreement with the experimentally determined values of Table 4 showing a maximum deviation of 9 MHz (less than 1.5%). We can thus infer that the actual geometries of the conformers are very close to those predicted ab initio (see Supporting Information).

The comparison between the theoretical and experimental values of the quadrupole coupling constants allows us to establish the orientation of the  $-\text{NH}_2$  group within the molecular frame and thus deduce the nature of the intramolecular interactions in which this functional group is involved. Since there is a maximum discrepancy of 13% between the ab initio and experimental values, the orientation of the  $-\text{NH}_2$  group can be established with small uncertainty. Given the orientation of the  $-\text{NH}_2$  group conformers AG and GG are mainly stabilized by an intramolecular hydrogen bond  $\text{O}-\text{H}\cdots\text{N}$  between the lone pair of the nitrogen atom and the hydrogen atom of the hydroxyl group (see figures in Table 4). In conformer GG an N-H bond points to the  $\pi$  cloud of the benzene ring, establishing an

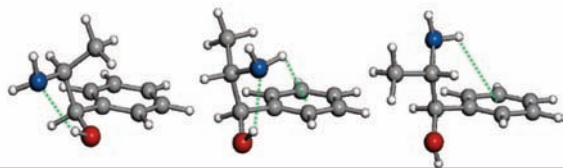


**Table 5.** Experimental Rotational and Quadrupole Coupling Constants for the Observed Conformers of Ephedrine (See Table S2 of the Supporting Information for a Complete Set of Parameters)

	AGa	AGb	GGa
A <sup>a</sup> /MHz	1998.63816(36) <sup>d</sup>	2115.87676(60)	1568.24542(47)
B /MHz	529.549516(44)	503.794270(41)	592.448481(69)
C /MHz	500.160018(43)	475.173400(51)	572.416000(73)
$\chi_{aa}$ /MHz	2.5350(14)	2.559(17)	2.4480(89)
$\chi_{bb}$ /MHz	-2.7448(19)	-4.621(11)	-3.2053(63)
$\chi_{cc}$ /MHz	0.2098(19)	2.062(11)	0.7573(63)
N <sup>b</sup>	87	83	98
$\sigma^c$ / kHz	1.3	1.3	1.9

<sup>a</sup> A, B, and C are the rotational constants and  $\chi_{aa}$ ,  $\chi_{bb}$ , and  $\chi_{cc}$  are elements of the  $^{14}\text{N}$  nuclear quadrupole coupling tensor. <sup>b</sup> Number of fitted hyperfine components. <sup>c</sup> Rms deviation of the fit. <sup>d</sup> Standard error in parentheses in units of the last digit.

additional N–H $\cdots\pi$  hydrogen bond. Conformer GA does not bear an O–H $\cdots\text{N}$  bond but it is stabilized by an N–H $\cdots\pi$  bond.

The intensities of several *a*-type transitions of AG and GA and *b*-type transitions of AG and GG have been compared to estimate the relative populations of the conformers in the jet assuming that all conformers are in their lowest vibrational state due to the cooling that occurs in the supersonic expansion. The line intensity is taken to be proportional to  $\mu_i \cdot N_i$ , that is, the corresponding electric dipole moment component (from Table 1) and the number density of the conformer in the supersonic jet. With these assumptions, a population ratio  $N_{\text{AG}}/N_{\text{GG}}/N_{\text{AG}} = 12:5:2$  is obtained. This can be taken as indicative of the conformer stability trend, which, on the other hand, is in good correlation with the ordering of their computed zero-point corrected relative energies (see Table 1). The unstrained AG conformer is reinforced by a strong O–H $\cdots\text{N}$  intramolecular hydrogen bond, appearing as the global minimum. Conformers GG and GA possess a less favorable folded arrangement. The GG form is more stable than GA due to the establishment of an O–H $\cdots\text{N}$  intramolecular interaction.

**b. Ephedrine.** EP presents six possible conformations (see Chart 1): two extended (AGa and AGb) and four folded (GGa, GGb, GAa, and GAb), which markedly differ in the value of their A rotational constants (see Table 2). The two extended conformers are nearly prolate asymmetric tops and should show the characteristic pattern of  $\mu_a$ -type, R-branch spectrum. Two sets of such transitions, with the typical quadrupole hyperfine structure of a single  $^{14}\text{N}$  nucleus, were detected. Their preliminary fits to the same Hamiltonian employed in the analysis of NEP led to initial values of the rotational constants and subsequent measurements of  $\mu_a$ -,  $\mu_b$ -, and  $\mu_c$ -type transitions with their corresponding quadrupole coupling components. The final experimental spectroscopic parameters are shown in columns 1 and 2 of Table 5.

The experimental values of the rotational constants are very close to those predicted ab initio for conformers AGa and AGb. The different disposition of one of the  $-\text{CH}_3$  groups causes a change in the orientation of the principal inertial axis system, which in turn results in significant differences in the rotational constants for AGa and AGb. This also causes the values of the quadrupole coupling constants  $\chi_{bb}$  and  $\chi_{cc}$  to become markedly different. We can thus unambiguously identify species 1 with

conformer AGa and species 2 with conformer AGb. In addition, no *c*-type transitions were detected for rotamer 2, which is consistent with the very small value of  $\mu_c$  predicted for this conformer (see Table 2). The microwave power used for optimal polarization of the different types of rotational transitions was in all cases in accordance with the electric dipole moment components predicted ab initio.

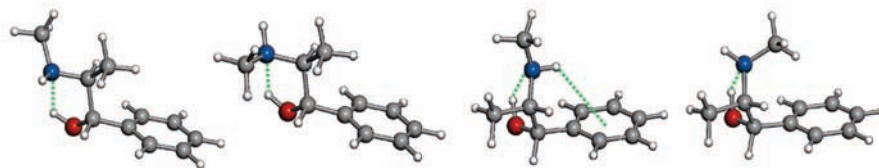
Considering the values of the dipole moment components of Table 2, wide frequency scans were conducted to search for *b*- or *c*-type transitions belonging to the folded forms (GG and GA), which led to finding a weak set of transitions that presented the quadrupole hyperfine structure caused by a  $^{14}\text{N}$  nucleus. Measurements of more  $\mu_a$ -,  $\mu_b$ -, and  $\mu_c$ -type transitions, and subsequent fits with the same Hamiltonian described above yielded the rotational and quadrupole coupling constants listed in column 3 of Table 5, which are only compatible with those predicted for the folded conformer GGa. Transitions attributable to other conformers of EP were not found after exhaustive searches in wide frequency regions. Since these conformers are predicted at higher energies with respect to the lowest energy conformer AGa, their rotational levels might not be sufficiently populated in our supersonic jet to allow the detection of their rotational transitions. The ab initio rotational constants of Table 2 are in excellent agreement with the experimental ones of Table 5, showing a maximum deviation of less than 1.5%. We can thus infer that the actual geometries of the conformers are very close to those predicted ab initio (see Supporting Information).

The intensities of several  $\mu_a$ -type transitions of each conformer have been compared to estimate the relative conformational abundances, and the same assumptions done for NEP have been applied. Using the values of  $\mu_a$  in Table 2, the population ratio  $N_{\text{AGa}}/N_{\text{GGa}}/N_{\text{AGb}} = 20:4:1$  is obtained. This indicates that conformer AGa is the most abundant species for EP, in agreement with the energy ordering predicted ab initio (Table 2).

In all three observed conformers the orientation of the  $-\text{NH}$  group makes possible the establishment of a N $\cdots\text{H}-\text{O}$  hydrogen bond between the hydrogen atom of the hydroxyl group and the lone electron pair of the nitrogen atom (see figures in Table 5). Conformers AGa and AGb are favored by an extended configuration of the side chain that diminishes steric impediments, although the methyl groups present a closer arrangement in AGb. In conformer GGa the more destabilizing folded

**Table 6.** Experimental Rotational and Quadrupole Coupling Constants for the Observed Conformers of Pseudoephedrine (See Table S3 of the Supporting Information for a Complete Set of Parameters)

	AGa	AGb	GGa	GGb
A <sup>a</sup> /MHz	2013.35560(27) <sup>d</sup>	2065.86584(17)	1645.9858(13)	1638.6903(23)
B /MHz	509.245110(80)	528.726489(56)	563.58807(46)	602.37256(22)
C /MHz	476.304851(82)	485.202523(53)	541.52877(47)	587.11272(25)
$\chi_{aa}$ /MHz	2.7231(78)	2.6577(48)	1.355(54)	1.987(70)
$\chi_{bb}$ /MHz	-4.5244(61)	-4.1185(40)	-0.329(34)	-0.185(46)
$\chi_{cc}$ /MHz	1.8013(61)	1.4608(40)	-1.026(34)	-1.803(46)
N <sup>b</sup>	66	55	19	22
$\sigma^c$ /kHz	2.1	1.2	4.1	2.5



<sup>a</sup> *A*, *B*, and *C* are the rotational constants and  $\chi_{aa}$ ,  $\chi_{bb}$ , and  $\chi_{cc}$  are elements of the <sup>14</sup>N nuclear quadrupole coupling tensor. <sup>b</sup> Number of fitted hyperfine components. <sup>c</sup> rms deviation of the fit. <sup>d</sup> Standard error in parentheses in units of the last digit.

arrangement of the side chain is counterbalanced by an additional N–H $\cdots\pi$  interaction between the H atom of the –NH group and the aromatic ring. The substantial contribution of the N–H $\cdots\pi$  bond in conformer GGa accounts for the higher stability of this form in comparison with conformer AGb.

**c. Pseudoephedrine.** PEP, similarly to EP, has six possible conformers (see Table 3) that can be classified into extended (AGa and AGb) and folded (GGa, GGb, GAa and GAb). The extended forms are expected to present the characteristic  $\mu_a$ -type, R-branch pattern of a near prolate asymmetric top. Two sets of such transitions showing the expected quadrupole hyperfine structure for a molecule with a single <sup>14</sup>N nucleus were first observed in the 6–8 GHz frequency region. Preliminary fits with the same Hamiltonian used for NEP and EP led to more measurements of *a*-, *b*-, and *c*-type transitions, each requiring polarization powers according to the predicted dipole moment components. Final fits of all measured hyperfine components yielded the parameters of columns 1 and 2 in Table 6. The combination of rotational and quadrupole coupling constants, as well as their comparison to those calculated ab initio, allowed us to unambiguously assign species 1 to conformer AGa and species 2 to conformer AGb of PEP.

Additional wide frequency searches for other conformers of PEP were conducted. After discarding transitions belonging to the AG forms, two new sets of *b*-type rotational transitions exhibiting <sup>14</sup>N quadrupole pattern were detected in the spectrum. Further measurements and fits of the observed transitions to the previously mentioned Hamiltonian gave the rotational and quadrupole coupling constants of columns 3 and 4 of Table 6. The values of the *A*, *B*, and *C* rotational constants of column 3 in Table 6 are very close to those calculated ab initio for conformer GGa (Table 3). Similarly, *A*, *B*, and *C* of column 4 in Table 6 are very close to those predicted for conformer GGb (Table 3). The experimental quadrupole coupling constants are also consistent with those predicted ab initio for conformers GGa and GGb. We can thus identify without doubt species 3 as conformer GGa and species 4 as conformer GGb of PEP. In agreement with the predicted values of the electric dipole moment components,  $\mu_a$ -type transitions have been detected for conformer GGb, while no  $\mu_a$ -type transitions have been observed for GGa. No unidentified lines remained in the PEP spectrum once these four conformers were assigned. The ab initio rotational constants of Table 3 are in fairly good agreement with

the experimental *A*, *B*, and *C* of Table 6, showing a maximum deviation of less than 2.5%. We can thus infer that the actual geometries of the conformers are quite close to those predicted ab initio (see Supporting Information).

Several *b*-type transitions of all detected conformers of PEP have been compared to estimate the relative conformational abundances making the same assumptions described for NEP and EP. Taking the values predicted theoretically for  $\mu_b$  (Table 3), the relative abundances  $N_{AGa}/N_{GGa}/N_{GGb}/N_{AGb} = 15:5:2:1$  are obtained. This shows that conformer AGa is the most abundant species in our molecular beam, which agrees with the ab initio calculations (Table 3). As it can be seen from the figures in Table 6, all detected forms of PEP are stabilized by an N $\cdots$ H–O bond between the lone electron pair of the N atom and the hydroxyl group. In conformer GGa the orientation of the –NHCH<sub>3</sub> group allows the establishment of an additional N–H $\cdots\pi$  interaction with the electronic  $\pi$  cloud of the benzene ring. This can explain why folded GGa is more stable than the extended AGb and folded GGb. The higher stability of conformer GGb with respect to AGb can be attributed to the less eclipsed disposition of the methyl groups since both conformers present an N $\cdots$ H–O hydrogen bond.

#### IV. Conclusions

The high resolution of the MB-FTMW technique allows independent analysis of the rotational spectra of individual conformers and to completely resolve the <sup>14</sup>N quadrupole coupling hyperfine structure, which conducts to a definitive identification of the different conformers of the neurotransmitters studied. Hence, three conformers of NEP and EP and four conformers of PEP have been unequivocally assigned through the analysis of their rotational spectra and the comparison of the experimental rotational and quadrupole coupling constants with those calculated ab initio. The advantages of this joint approach are clear: theory guides experiment by providing predictions of the pertinent molecular properties and experimental data constitute a solid and appropriate reference for theory.

The conformational preferences showed by these three neurotransmitters can be rationalized in terms of the various intramolecular forces at play: hydrogen bonds involving the –OH and/or the –NH groups and steric interactions between

the two methyl groups. All the observed conformers present an intramolecular hydrogen bond O—H···N between the lone pair of the nitrogen atom and the hydrogen atom of the hydroxyl group, except the higher-energy conformer of NEP (see figures in Tables 4–6). The O—H···N bond is thus the main stabilizing contribution to the conformational energy. The other intramolecular interactions that take place within each conformer add to the O—H···N interaction further modulating and determining the ultimate relative stability of the different conformers.

A common feature to all neurotransmitters here is that their most stable conformer corresponds to the AG family: AG in NEP and AGa in EP and PEP. In these conformers the side chains adopts an extended disposition which minimizes steric impediments. The next conformer in abundance, again for the three neurotransmitters, belongs to the GG family: GG in NEP and GGa in EP and PEP. In these conformers an interaction between the —NH group and the  $\pi$  cloud of the aromatic ring counteracts the less favorable folded disposition of the side chains stabilizing them with respect to the AGb forms, which present extended side chains like conformer AGa but with a closer arrangement of the methyl groups. Conformer GGa for EP had not been detected before using IR ion dip spectroscopy and UV hole-burning techniques.<sup>5,6</sup> These techniques can sometimes fail to detect conformers with a short-lived excited electronic state, as it has happened for guanine.<sup>20</sup> The identification of the GGa conformer changes the former picture of the conformational landscape of EP where conformer AGa overwhelmingly dominated the spectrum to a new landscape where AGa is still predominant but it is just five times more abundant than conformer GGa. The third conformer in abundance in EP and PEP corresponds to the AGb and GGb forms, respectively. Notice that the change in the chirality of one center in going from EP to PEP forces a different arrangement of the amino and methyl groups. This causes the AGb conformer to have a more strained disposition of the methyl groups for PEP.

Investigations in the gas phase provide the basic knowledge of the inherent shape of chiral compounds and the intramolecular

forces that control the conformational preferences. Further studies can then be addressed to investigate the effect of adding individual water molecules (microsolvation) to mimic the transition to the biological medium, where intermolecular interactions with solvent molecules also affect molecular shape. Investigations using UV resonant two-photon ionization and IR ion-dip spectroscopies, and laser-induced fluorescence<sup>21</sup> have detected 1:1 and 1:2 clusters of EP and PEP with water, and significant differences in the conformational landscape of PEP have been observed upon hydration, although in some cases the assignment was not conclusive. Rotational spectroscopy has been successful in identifying 1:1 and 1:2 complexes of biological molecules,<sup>11,22–24</sup> and in some cases it has been possible to provide data on cooperative effects in the 1:2 complexes. Its application to the study of microsolvation of neurotransmitters could shed more light on the subject and, particularly, it might detect conformers of the 1:1 and 1:2 complexes of EP-water where the AGa form of EP participates.

**Acknowledgment.** This work has been supported by the Dirección General de Investigación (Ministerio de Educación y Ciencia, Grant No. CTQ2006-05981/BQU), and the Junta de Castilla y León (Grant No. VA012 C05). V.C. thanks the Ministerio de Educación y Ciencia for an FPI grant.

**Supporting Information Available:** Tables of the rotational frequencies of the conformers detected for NEP, EP, and PEP measured in this work together with the complete set of rotational constants determined from the fits, and ab initio geometries predicted for the observed conformers of NEP, EP, and PEP. This material is available free of charge via the Internet at <http://pubs.acs.org>.

JA807674Q

(20) Mons, M.; Piuze, F.; Dimicoli, I.; Gorb, L.; Leszczynski, J. *J. Phys. Chem. A* **2006**, *110*, 10921, and references therein.

- (21) Butz, P.; Kroemer, R. T.; Macleod, N. A.; Simons, J. P. *Phys. Chem. Chem. Phys.* **2002**, *4*, 3566.  
(22) Blanco, S.; López, J. C.; Lesarri, A.; Alonso, J. L. *J. Am. Chem. Soc.* **2006**, *128*, 12112.  
(23) Alonso, J. L.; Cocinero, E. J.; Lesarri, A.; Sanz, M. E.; López, J. C. *Angew. Chem., Int. Ed.* **2006**, *45*, 3471.  
(24) Melandri, S.; Sanz, M. E.; Caminati, W.; Favero, P.; Kisiel, Z. *J. Am. Chem. Soc.* **1998**, *120*, 11504.